ACS APPLIED MATERIALS & INTERFACES

Review

www.acsami.org

Mechanical Stability of Surface Architecture—Consequences for Superhydrophobicity

Brendan P. Dyett,[‡] Alex H. Wu,[‡] and Robert N. Lamb*[,‡]

School of Chemistry, University of Melbourne, Parkville, Victoria, Australia, 3010

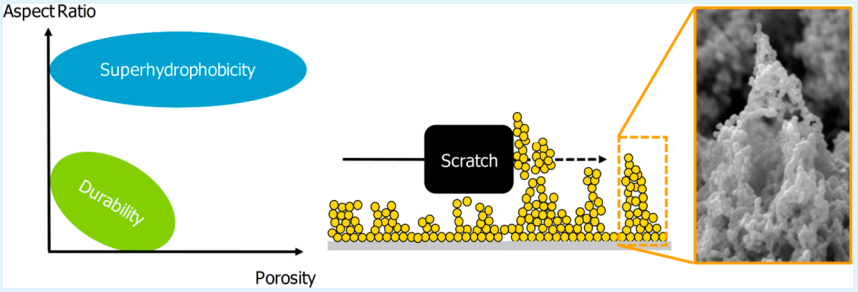

ABSTRACT: Wet chemistry methods such as sol−gel provide a facile means of preparing coatings with controlled surface chemistry and architecture. The manipulation of colloidal "building blocks," film constituents, and reaction conditions makes it a promising method for simple, scalable, and routine production of superhydrophobic coatings. Despite all of this, the practical application of superhydrophobic coatings remains limited by low mechanical durability. The translation of chemistry to mechanical strength within superhydrophobic films is severely hindered by the requisite physical structure. More specifically, porosity and the surface architecture of roughness in sol−gel-derived films contribute significantly to poor mechanical properties. These physical effects emphasize that collective structure and chemistry-based strategies are required. This challenge is not unique to superhydrophobics, and there are many principles that can be drawn upon to greatly improve performance. The delicate interplay between chemistry and physical structure has been highlighted through theory and characterization of porous and rough interfaces within and outside the framework of superhydrophobics. Insights can further be drawn from biology. Nature's capacity for self-repair remains extremely challenging to mimic in materials. However, nature does demonstrate strategies for structuring nano- and microbuilding blocks to achieve generally mutually exclusive properties. Difficulties with characterization and example mechanical characterization methods have also been emphasized.

KEYWORDS: *superhydrophobic, review, durable, structure, needle, crater, sol−gel, biomimetic*

1. INTRODUCTION

Superhydrophobicity, defined as exhibiting water contact angles exceeding 150° and rolling angles less than 5°, is accompanied by a myriad of potential applications including self-cleaning,[1] anti-icing,[2] and the prevention of marine biofouling.[3,4] An understanding of this behavior can be described by Young,[5] Wenzel,[6] and Cassie and Baxter;[7] with the latter now used extensively.[8] Both Wenzel and Cassie−Baxter models describe the enhancement of nonwetting properties through surface roughness, and hence development of surface structures to yield superhydrophobicity has been a prominent area of research for some time.[9,10] In particular, Cassie−Baxter illustrates the development of a composite air−solid surface with sufficient surface roughness, greatly reducing solid contact points and thus adhesion of water droplets.[11] However, this reduced contact area also introduces fragility upon mechanical load whereby the true area of contact is substantially reduced yielding high contact pressures exceeding the materials mechanical properties.[12] As a consequence such structured surfaces are highly prone to abrasion and rapidly lose superhydrophobicity as a result of mechanical damage to surface features and ensuing smoothening of the interface. The mechanical frailty of these surfaces is a primary drawback for many practical applications.[13] While wetting studies and general preparation methods have been and continue to be reported, the mechanical durability is frequently overlooked. Yet the fundamental understanding of this problem is vital to achieving durable surfaces and thus any widespread practical applicability.

The eventual properties of a film will inherently depend on its manufacture. To induce superhydrophobicity a process that both generates surface roughness and alters surface chemistry is necessary. Numerous procedures have been reported to prepare superhydrophobic surfaces. Of these, two broad categories are considered to be "top-down" or "bottom-up". Top-down denotes methods of inducing roughness by removing material from a bulk matrix—such as patterning by lithography[14] or etching techniques.[15] Conversely, bottom-up describes roughness and functionality constructed from the substrate upward, typically as a thin film, through methods such as crystal growth,[16,17] layer-by-layer,[18] chemical vapor deposition,[19]

Received: June 27, 2014
Accepted: October 15, 2014
Published: October 15, 2014

 © 2014 American Chemical Society dx.doi.org/10.1021/am505487r | *ACS Appl. Mater. Interfaces* 2014, 6, 18380−18394

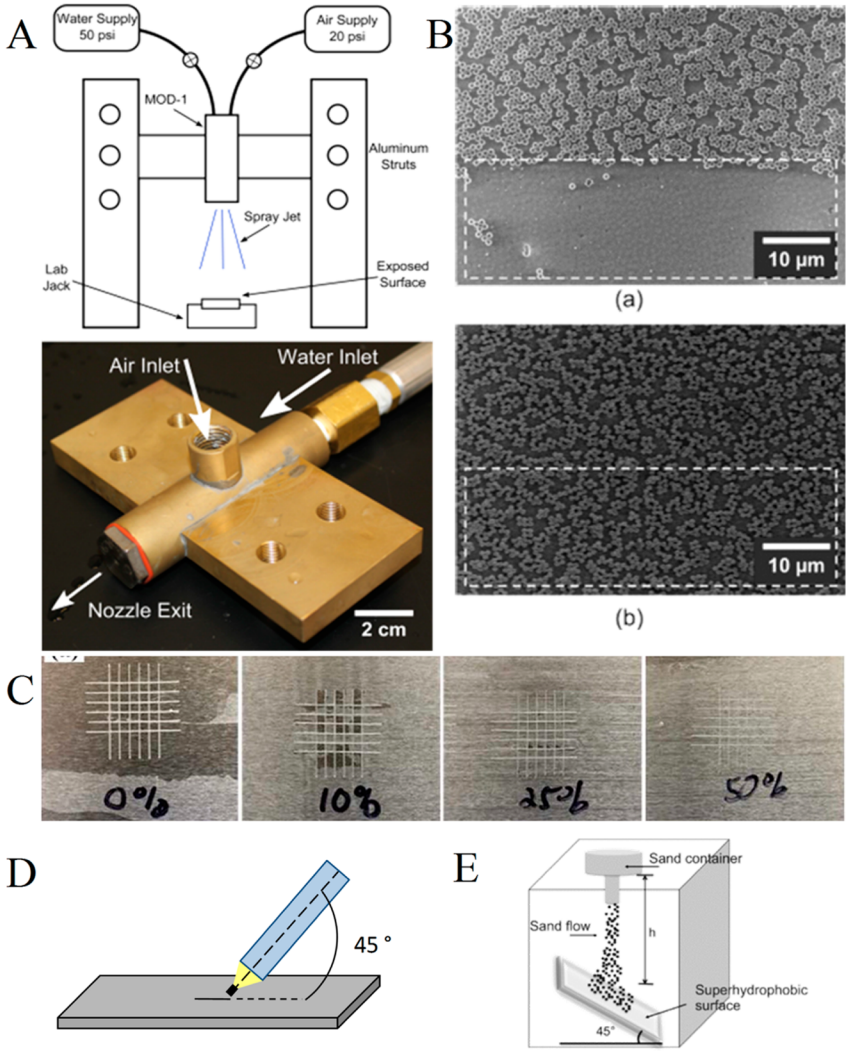

Figure 1. (A) (upper) Schematic and (lower) photograph of water-jet abrasion setup reproduced from Davis et al.[33] Copyright © 2014 American Institute of Chemical Engineers (B) SEM of surfaces prepared by Deng et al.[35] after tape-adhesion tests prior to and after covalently binding to substrate. Copyright 2014 Wiley-CH Verlag GmbH & Co. KGaA, Weinheim. (C) Example cross-hatch testing performed by Sparks et al.[42] with varying degrees of removal. Copyright 2014 American Chemical Society. (D) Illustrated schematic of pencil hardness tests. (E) Schematic of sand abrasion test driven by gravity, as performed by Deng et al.[35] Copyright 2014 Wiley-CH Verlag GmbH & Co. KGaA, Weinheim.

electrospinning,[20] and sol–gel. Extensive reviews regarding preparation of superhydrophobic materials have previously been reported.[10,21,22] While bottom-up strategies are generally more versatile, many techniques can be limited by costs, scale, and substrate constraints. Sol–gel processing is advantageous owing to facile customization and scalability in terms of tailoring chemistry toward prescribed properties[23] and applicability to most substrates.

With a specific focus on solution-based sol–gel-derived coatings it will be demonstrated through conventional porosity, beam models, and existing reports that regardless of chemical strategies, the physical structure is paramount to achieving mechanically durable surfaces. This will be further emphasized through the hierarchical structuring of natural materials. While there is a focus toward wet chemistry/bottom-up constructed surfaces, many studies below are theoretical or produced via lithographic means owing to higher reproducibility.[22] Even so, their findings still hold relevance to understanding and determining structural integrity. Further, as correlations are drawn toward sol–gel preparation, they may hold relevance to other means of surface construction.

In parallel with the difficulty preparing mechanically robust superhydrophobic films, superhydrophobic films are intrinsically nonideal samples for mechanical characterization. There is a need to universally adopt methodology beyond pencil hardness and similar techniques. The applicability of tribological principles in wear and characterization to these films will be also emphasized.

2. THE BROAD SCOPE OF DURABILITY AND CHALLENGES IN CHARACTERIZATION

Beyond the overall outcome of achieving durable and nonwetting surfaces, characterizing these films is a challenge in itself. The studies explored below will largely consider material properties such as Young's Modulus, E; however, determining such parameters can be complicated. In fact, despite the practical importance, systematic quantification of durability of superhydrophobic films has been scarce and focuses on the wettability rather than on the long-term stability. This issue is noted in a review by Verho[13] and more recently by Xue.[24] This is particularly true when durability is narrowed

further to only consider mechanical properties, which is the primary scope of this report. In particular, the preservation of surface roughness against compressive and abrasive or shear forces[25] is of utmost importance.

Admittedly, mechanical durability is not the only aspect of durability. The many other perspectives of interest toward the robustness of these films includes long-term submersion, water droplet impact, stability to UV,[26] extreme pH, and solvent environments. These issues have been collated in a recent report by Malavasi et al.[27] This report encompassed proposed protocols for the standardized testing toward these factors are evaluated by preservation of the receding contact angle after cycles of each test. In general, stability of coatings against factors such as pH or solvents can be greatly improved by fluorination, which simultaneously improves nonwetting properties. For particular applications regarding wetting resistance, long-term submersion and droplet pressure, work presented by Extrand,[28] Tuteja et al.,[29] and Zhao et al.[30] is particularly interesting. In some cases the presence of a water droplet may induce structural change due to capillary pressure. This has been demonstrated for high aspect ratio fibrillar structures.[31] Damage to very fragile particulate films due to similar effects may also be expected; however, to our knowledge this has not been extensively discussed. This report will assume higher performance in mechanical tests should reflect resistance to these effects. As structures increase in stiffness and repellency this effect becomes less pronouced.[32]

2.1. Mechanical Robustness. Any loss or change in surface roughness will alter performance in other tests. Abrasion may cause a loss of aspect ratio impacting wetting or alter surface chemistry. In this sense the longevity in practical application is directly tied to mechanical durability, which still remains the main practical hurdle to application. This was demonstrated by Malavasi et al.[27] where the abrasion test had the most profound impact in their standardized testing. In this case abrasion was caused by a water-jet test similar to tests performed by Davis et al.[33] and Jung and Bhusan.[34] In these tests the water pressure and stream−substrate distance and angle are determining factors in how the substrate is abraded. As the impact pressure is increased or applied in repeated cycles, one would expect increased abrasion to the surface. Sand abrasion is a similar test where sand grains are dropped from a height onto the titled surface.[35] The contact loadings can be calculated from drop height, gravity, particle size, and density. In many cases material spanning kim-wipes to sandpaper is rubbed across the surface.[36,37] These are generally observed qualitatively or accompanied by a calculated loading pressure from either touch or set weights. For tests including pencil hardness,[38] cross-hatch,[39] or tape adhesion[40,41] there are typically American Society for Testing and Materials (ASTM) guidelines. In pencil hardness tests a range of pencils spanning 9B (soft) to 9H (hard) are run across the surface until a pencil fails to either scratch or gouge (delaminate) the film. These ratings are then referred to as scratch or gouge pencil hardness (not to be confused with material property hardness). Depending on the ASTM procedure following the loading, scratch length and requirements for a pass may vary. Cross-hatch and tape adhesion are performed utilizing specific tape brands, which are applied to the surface and subsequently removed. Cross-hatch tests involve the scratching of the target region of the film into a square grid or an X prior to the adhesion test. Depending on the ASTM procedure the brand of tape, adhesion time and pass grading may alter. Gradings are typically based upon the regions removed, that is, complete removal, removal at scratch lines, no removal, etc.

The majority of procedures employed (illustrated in Figure 1) could be considered macroscale techniques emanating from industrial coating characterization. These techniques offer many advantages in cost and time efficiency. In particular, they are readily accessible to most laboratories, though obviously some laboratories prefer differing methods. These methods are typically validated with wetting angles from which nano- or microdamage can be inferred. Moreover, in combination with electron microscopy, very practical data regarding structure performance can be rapidly attained. There is a tendency for most reports to encompass only one or two of these tests, which limits comparison between reports. More so, these tests are highly variable from factors such as human error, tape model, pencil model, water pressure, dropping height, etc., which all must be identical for true comparison.

2.2. Nanoindentation. Justification for the broad adoption of these techniques discussed above may stem from the difficulties in utilizing characterization on relevant length scales. To improve understanding in a scientific context more sensitive methods to quantify material properties would be ideal. When probing nanoscale features such as those present on superhydrophobic films it would be desirable to utilize relative length scale techniques such as nanoidentation.[43−45] A nanoindenter or atomic force microscopy (AFM) is able to record the dynamic displacement of a tip through a material, and the corresponding curve will directly reflect the mechanical properties of the material. Resultant displacement versus load graph and area of the indent can be utilized to determine material properties. The analysis of depth-sensing nanoindentation is unfortunately complicated by the presence of surface roughness due to challenges in determining the contact area between the indenter and the surface,[46] illustrated in Figure 2. This can lead to dramatic scatter of calculated results. From a basic starting point, film penetrations are usually at a low (<10) percentage of film thickness to avoid substrate influence. At the same time, to avoid the scattering from roughness, indents are performed to a depth of $20R_a$.[46] It is immediately apparent that thin superhydrophobic films are not ideal for these measurements. Thus, the application to superhydrophobic films is nontrivial; however, the parameters are imperative in rationalizing coating performance. Procedure and analysis of nanoindentation experiments has been developed by Doerner and Nix[47] and by Oliver and Pharr.[48] Joslin and Oliver[49] have further developed a procedure more suited to rough surfaces; a succinct review on nanomechanical characterization is provided by Bhushan[50] and recently by Palacio and Bhushan.[51] At shallow penetration depths employed to study rough films additional concerns are substrate influences,[46,50] scale effects,[52−55] and surface effects.[56] Scale dependence of nanostructures is noted further below.

For structures similar to those in Figure 2, standard approach procedures in indentation experiments may result in difficulties detecting the surface, and subsequently samples may be damaged initiating contact. This has been improved upon by a hybrid nanoindentation technique utilizing alternating current force modulation, demonstrated by Asif et al.;[57−59] Dynamic stiffness measurements yielded enhanced sensitivity to detecting and determining mechanics of surfaces. This avenue may prove more applicable to displacement studies of highly rough surface features.

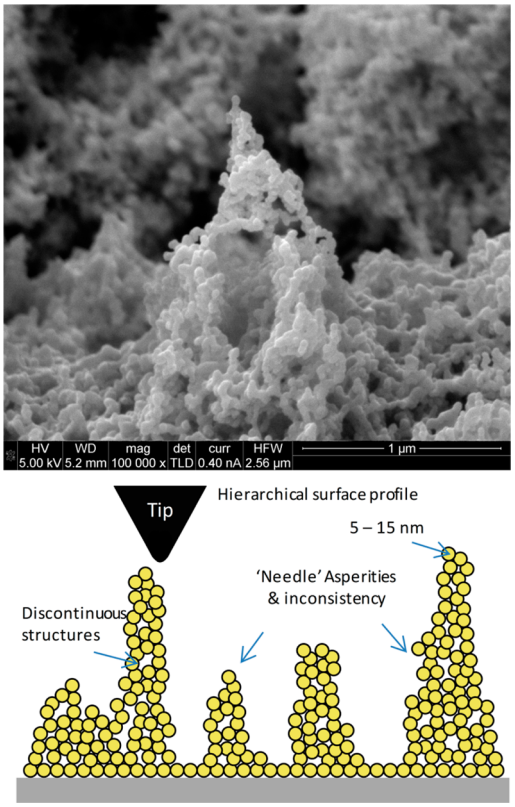

Figure 2. (upper) SEM of isolated "needlelike" sol–gel film prepared from the aggregation of silica nanoparticles. Similar structures with varying dimension are also present in fore- and background. (lower) Idealized schematic representation of a sol–gel-derived superhydrophobic film. The surface exhibits multiscale roughness on similar and greater scale to the indentation tip, discontinuities (pores) within the structures, and nonuniformity between surface features. Such variation in contact area between the tip and the surface leads to high scatter in calculated material properties.

An additional notable technique is the in situ indentation of structures within scanning electron microscopes (SEMs). Owing to the demand for miniaturization of electronic materials, metallic nanorods and wires have received extensive attention to their mechanical properties utilizing this technique. Subsequently, there is a multitude of studies analyzing the compression of metal pillars.[60−62] This technique allows for high-resolution visual interpretation and studying dynamic failure events of local structures. Philippe[63] demonstrates the manipulation of a single nanowire bending upon strain induced by an AFM tip, Figure 3. Precise manipulation allows for dynamic capture of events and offers vast information regarding the failure of nanostructures.

A review of in situ indentation techniques has recently been reported by Nili.[64] To our knowledge, this is a technique that is yet to be employed in the study of superhydrophobics. Despite the increased challenge that would arise with navigating ultrarough surfaces such as attempting to land on single asperities, this technique provides visual and quantitative means to identifying and addressing the failure mode of nanostructures employed within superhydrophobics. Of particular interest would be determining the extent to which desired material properties are maintained from film precursors to surface structures and the influence on the dynamic failure of the structure.

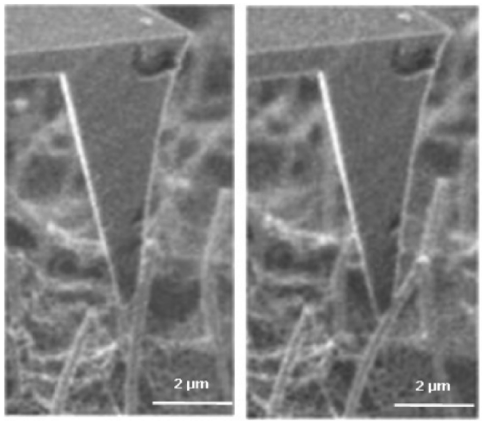

Figure 3. AFM tip employed for in situ bending experiments of rhenium nanowires. Reproduced with permission from L. Philippe, I. Peyrot, J. Michler, et al., *Appl. Phys. Lett. 91*, 111919, **2007**.[63] Copyright 2007 AIP Publishing.

2.3. Nanoscratching and Friction. Performed in a lateral direction, indentation allows for micro and nanoscratch experiments, which can be more readily interpreted allowing qualitative trends to be developed. To an extent, this avoids some of the strenuous experiment or analysis accompanied by indentation. The scratch behavior can be influenced by tip geometry and normal load.[50] These experiments can provide crucial understanding toward improving the abrasive resistance of surface micro- and nanostructures. By simultaneously performing a scratch and monitoring the friction coefficient, mechanistic information can be inferred regarding the failure of the surface asperities.[65−67] Throughout application, the interface will experience diverse loads with both normal and lateral components. In this sense, scratch tests are perhaps more meaningful to determine durability through determining resistance to shear forces and wear at multiple length scales. Jung and Bhushan[34] demonstrate the characterization of superhydrophobic films prepared through lithographic and spray methods utilizing AFM. In contact mode, a 15 μm borosilicate sphere was scanned at very low loads (100 nN) across the surface. A similar experiment was performed using a 3 mm Sapphire ball at 10 mN. Variation in height scans before and after wear scanned allowed damage to be inferred, in this case comparison between surfaces of epoxy-nanotube composite and lotus wax.

Beyond performing tests, rationalizing which mechanical properties are desirable may not be immediately clear. Ideally, the chemistry can readily be manipulated to engineer material properties; however, the extent to which these properties translate in surface structures may be limited, particularly in porous or fine structures. This is discussed later in the review. The material property hardness (H) can be interpreted in a number of ways. Within this report hardness will be discussed broadly as a measure of the material's capacity to resist permanent deformation from an opposing load. Examples below will use specific values referring to indentation hardness. From the definitions of the term, hardness is an ideal trait for surface structures. However, materials with high hardness may be too brittle and rapidly fail above the materials yield stress, even more so considering amplified contact pressures. Conversely, materials too soft may succumb to effects such as capillary forces between asperities.[31] For rationalizing wear behavior, it has been reported the ratio H/E may be more

relevant. This term is a descriptor of the limit of elastic behavior of the material. Similarly, the term H^3/E^2 can provide insight into yielding behavior of the material; high values indicate elastic, while low values indicate plastic behavior.[68,69] Accordingly, through the determination of material properties H and E, mechanical properties can be correlated to their performance in mechanical tests such as scratching. Note that through this methodology, the elastic modulus is reduced, that is, becoming less stiff. This is in contrast to the conventional approaches to strengthen materials, which is to increase the rigidity of individual structures through methods such as cross-linking.

An interesting example encompassing these wear principles is provided by Skarmoutsou et al.[70] studying the mechanical properties of textured poly(methyl methacrylate) (PMMA) induced by oxygen plasma. The material properties were determined through nanoindentation methods and then correlated to nanoscratch behavior. The wear performance of surfaces was rationalized through analysis of friction behavior and material H/E and H^3/E^2 ratios. A reduced data set is provided in Figure 4 where it was shown that with high surface roughness there was a significant decrease in mechanical properties H and E. Furthermore, from property ratios H/E and H^3/E^2 it was demonstrated that the rough surfaces exhibited reduced wear resistance and increased plastic behavior, respectively; both unfavorable for maintaining surface geometry. This is further demonstrated through simultaneous scratch and friction testing. Friction, a measure of resistance of surfaces moving against each other, is thus highly dependent on surface topology. Illustrated in Figure 5, the friction force becomes increasingly nonlinear with normal load on the textured sample. Considering Coulombs law of friction, friction force = μF_{normal} (F_{normal} denotes the force normal/perpendicular to the surfae), where μ is the friction coefficient (gradient), μ represents the friction modes during the scratch and should remain constant (linear) if adhesion remains the only contributor to friction. This trend, exhibiting a variable gradient (μ) as a sharpening of the trend, is clearly evident. This increase in friction is interpreted to result from the energy absorbed during plastic deformation (plowing) of surface asperities. Thus, as well as adhesion, there is a plowing factor contributing to the friction coefficient with increasing load. This example demonstrates how the complementary analysis of both mechanical properties and scratch behavior can provide understanding of the mechanisms of failure of superhydrophobic surfaces. Recently, a similar study was reported from the same research groups.[71] This methodology exemplifies a relevant length scale technique for the mechanical characterization of these films.

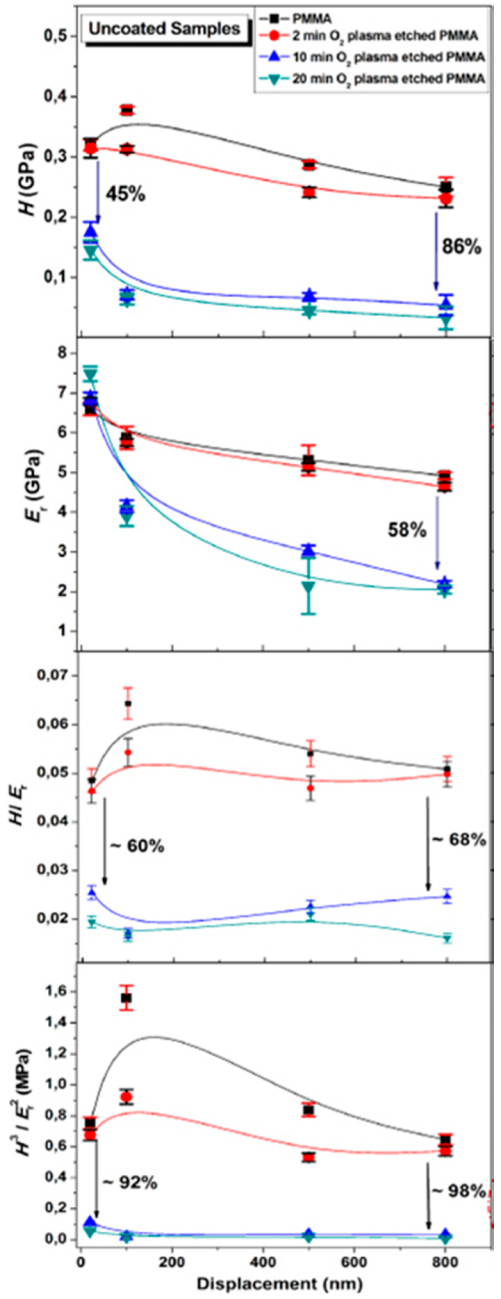

Figure 4. Hardness (H) and Young's modulus (E) values determined through nanoindentation methods on smooth and plasma roughened PMMA. Plasma etching increasingly roughens the PMMA with time. Wear resistance is determined through H/E ratio, and plasticity as H^3/E_r^2 are also plotted. Reproduced with permission from A. Skarmoutsou et al., **2012**, *Nanotechnology*, *23*, 505711.[70] Copyright 2012 IOP Publishing.

3. SOL–GEL CONSTRUCTION OF SUPERHYDROPHOBIC FILMS

From the previous section, sol–gel-derived superhydrophobics were introduced in Figure 2 as challenging materials for characterization. Sol–gel is a frequently utilized wet chemistry approach for the production of roughened or porous frameworks, and despite characterization challenges, there are many also many advantages. Conceptualized as a "building block" approach, sol–gel allows for fine control over surface topology and chemistry through manipulating the sol constituents and reaction conditions.[72] A typical procedure comprises the preparation of a colloidal solution whereby in situ gelation occurs via covalent and physical bonding between inorganic particles and binder matrix/precursors.[73] During deposition of the colloidal mixture the particles aggregate to form hierarchical roughness as illustrated in Figure 6, while binding agents act to interconnect between particles and adhere to the substrate.

Mechanical durability issues in sol–gel-derived coatings emanate from the manner in which particles aggregate during deposition. While many studies have reported improved mechanical and thermal properties of materials upon the addition of nanoparticles,[76−80] these improvements, referred to

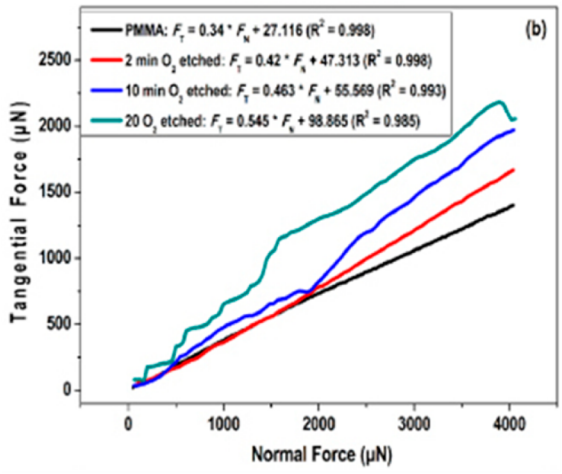

Figure 5. Friction force vs normal load for smooth and roughened PMMA substrate. The increasing nonlinear trend for the roughened sample indicates plastic deformation through plowing of surface asperities. Reproduced by permission of A. Skarmoutsou et al., **2012**, *Nanotechnology*, *23*, 505711.[70] Copyright 2012 IOP Publishing. All Rights Reserved.

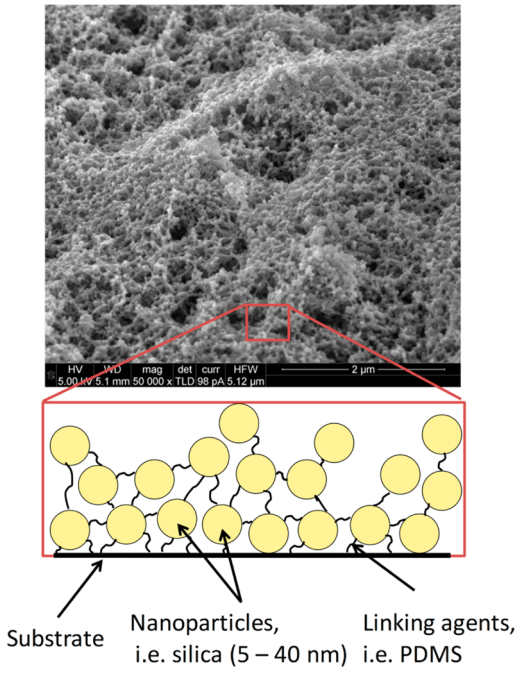

Figure 6. SEM image of superhydrophobic surface prepared through sol–gel preparation, coupled with idealized schematic of example sol–gel preparation of superhydrophobic coatings derived from the aggregation of silica nanoparticles, bridged covalently by PDMS chains.[74,75]

as the "filler effect," are achieved at low particle loading, often as low as 0.1%.[81] The positive reinforcement of this effect is strongly dependent on interfacial interaction and therefore highly dependent on the surface properties of filler and matrix utilized.[76−78,80] At high loadings, particles become a substantial film component, resulting in particles interacting with themselves rather than the polymer matrix, disrupting material properties.[77,81] At particle loadings sufficient to generate surface roughness that is required in superhydrophobic coatings this effect is no longer present, and at this loading particles are in fact detrimental to the properties of the material. In effect, such a film will become very brittle, with the weakest fracture points existing between particle agglomerates.

To enhance durability it is desirable to increase linkages between particles through chemical bonding. Covalent bonds can be introduced between particles to impart more improved physical traits than physical binding.[75] This procedure was first reported by Zhang et al.[82] in a 1997 patent. Many similar procedures have subsequently been reported in open literature. In general variations primarily exist in the organic functionality of the linking agents used. Example functionalities explored include epoxy–amine,[83,84] acrylate,[85] silanes, and siloxanes.[75,86,87] A range of other chemistries have also been explored.[10,88−91] Typically, the utilization of advantageous high strength bonds is inherently limited due typical hydrophilic character.[37] Conversely, use of hydrophobic terminal groups (i.e., alkyl) inhibits networks and induces porosity,[92] a difficulty discussed below. These linkages are also limited by the particle loading required and the degree to which intrinsic bulk properties are reduced at high particle loading. This is an important consideration as an increase in linking agents effectively smoothes the surface, Figure 7.

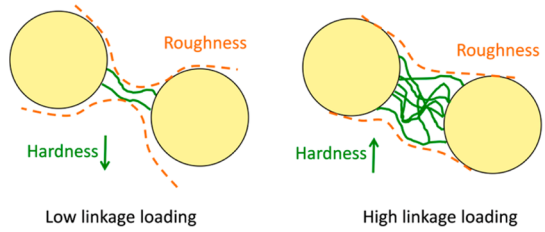

Figure 7. Idealized schematic of the inverse relationship between cross-linking and surface roughness.

The scope of chemistry already explored is indicative of overarching limitations such as those frequently overlooked regarding the geometry of surface roughness. As discussed, the aggregation of particles typically yields "needlelike" structures with considerable edge effects.[65] This structure is desirable for minimizing solid–water interactions; however, it is limited in durability.[11] The reduced contact area from needlelike architectures ensures high contact pressures and are readily abraded, increasingly so beyond the yield stress of the material. In this regard, surface architecture of superhydrophobic coatings typically presents a compromise between surface wettability and mechanical properties.

Promising alternatives are "craterlike" structures, where roughness does not protrude per se but represents a voids/pore network across a planar film. In a procedure similar to the one above, sol–gel synthesis was employed to create a gel; however, roughness was engineered not primarily through particle aggregation but through the removal of a sacrificial template.[38] Akin to those of needlelike structures, the properties of these structures can be tuned through altering linking groups. These structures exhibit increased solid area to distribute load and improved lateral stability compared to structures exhibited in Figures 2 and 6. Despite yielding substantially higher abrasive resistance, these films have surprisingly received quite minimal attention with only few publications further exploring crater roughness.[93−99] Recently, additional research exploring similar morphologies were reported, namely, a sol–gel preparation[100] (Figure 8) and

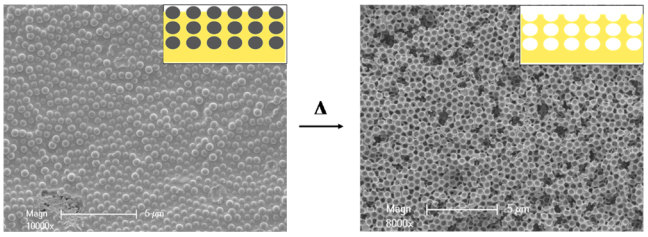

Figure 8. SEM and overlay schematic of the preparation of a porous craterlike surface through the thermal decomposition of polymer spheres within a methyltrimethoxysilane matrix. Reproduced with permission from B. P. Dyett, A. H. Wu, and R. N. Lamb, *ACS Applied Materials & Interfaces*, Article ASAP. Copyright 2014 American Chemical Society.[100]

lithographic/molding prepration.[101] The latter provides an exemplary figure modeling the contrast between protruding and holelike asperities. The stress distribution calculation for an individual cone and inverse cone is reproduced in Figure 9.

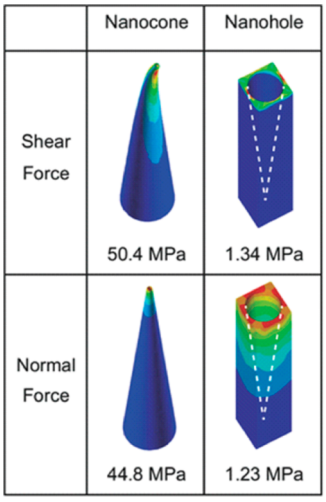

Figure 9. Stress distribution calculation by finite element method, exemplifying the contrast between protruding needlelike features and hole- or craterlike features under equivalent loading. A loading of 4 N across 5 mm radius circular area was chosen to simulate a finger brushing across the textured polyurethaneacrylate (E = 400 MPa). Reproduced with permission from J. G. Kim, H. J. Choi, K. C. Park, R. E. Cohen, G. H. McKinley, and G. Barbastathis (2014), DOI: 10.1002/smll.201303051. Copyright 2014 Wiley-CH Verlag GmbH & Co. KGaA, Weinheim, Germany.[101]

From further comparison below it can be further demonstrated that the exploration and control of different architectures hold critical importance to bridging dichotomy between roughness and durability.

4. POROSITY

"Needlelike" and "craterlike" structures in a broad sense can be considered as simply mesoporous and macroporous bodies, where porosity is defined in eq 1. Needlelike structures are essentially nonclose packed stacking of spheres with substantial voids between asperities, and craterlike is analogous to honeycombs or foams.

$$\text{porosity} = 1 - \frac{\rho_{\text{sample}}}{\rho_{\text{bulk}}} \tag{1}$$

Many porous materials akin to honeycomb and foams have been termed "cellular solids" and exhibit structures that are desirable for diverse applications owing to their lightweight, high surface areas, and tunable thermal and mechanical properties.[102] The mechanical properties of these porous materials have been studied extensively at the macroscale, and a number of porosity theorems have been developed, which subsequently could provide perspective on superhydrophobic films. Previously, two material properties were introduced for interpreting wear behavior. In this discussion particular importance is again placed on mechanical properties hardness (H) and elastic modulus (E).[50] In this application the yield stress is also important. Classically for basic open and closed cell foams a direct power-law relationship can be applied between the mechanical properties of a solid material and that of the same material with a degree of porosity, eq 2.[102,103]

$$E_{\text{film}} = E_{\text{ref}}\left(\frac{\rho_{\text{film}}}{\rho_{\text{ref}}}\right)^{n} \tag{2}$$

where E and ρ refer to elastic modulus and density, respectively; subscript film refers to a porous film and ref denotes a reference solid material; and exponent n is dependent on the failure mechanism. This model was adapted to allow modeling of porous structures that deviate from simple open/closed foams, eq 3.[104]

$$\frac{A}{A_0} = (1 - aP)^{n} \tag{3}$$

where A and A_0 represent the material property of a porous and nonporous sample, and α and f are fitting parameters; material constant, a, describes the packing geometry factor, while n describes the pore geometry as above. These predictive models can be adapted to fit multiple mechanical properties[105] and subsequently applied to describe smaller-scale influences of structure including ratio of wall thickness between pores to pore diameter[102,103] as well as interconnectivity driven by pore wall imperfections.[106,107] Bellet[108] demonstrated as the porosity of silicon was increased to 90% the modulus was reduced by 2 orders of magnitude. Diverse examples of application are reported.[104,106,109−111] While the power-law, eq 2, cannot be quantitatively assumed without comprehensive understanding of the structure[103] it does provide some insight into what properties one can expect in engineering porous films.

The minimum solid area model is also used to describe properties of porous materials[112−114] describing relationships of a number of material properties such as hardness, compressive strength, wear, tensile strength, etc., by

$$A_{\text{poroous}} = A_0 e^{-bp} \tag{4}$$

where A_{porous} is a property of a porous material, A_0 is the property of the corresponding nonporous material, b is a parameter that reflects the character of porosity and the property being measured (i.e., compressive or tensile), and p indicates the volume fraction porosity. The character of the pores describes whether they are present as spherical or cylindrical pores within a matrix or pores between stacked particles. Depending on the stacking of particles or the ordering of the pores, b will either increase or decrease.[113] This model may be more appropriate for needlelike coatings, which are essentially randomly stacked particles and craterlike coatings, which are essentially spherical pores within a matrix. It is

important to note that this model can be valid for only certain porosity ranges if changes in the stacking of particles/pore (value of b changes) occur with changing porosity.[110] Diaz and Hampshire[109] demonstrate that eqs 3 and 4 can be utilized to describe Young's modulus of silicon nitride, describing Young's modulus halving across 0−25% porosity.

From eqs 2−4 it is shown that mechanical properties are inversely proportional to a power-law of porosity. These porosity models have been employed for a diverse range of structured surfaces outside the niche focus of superhydrophobics including porous silica[110,115] and anodized aluminum.[116−119] Notably, in the pursuit of low dielectrics, porous materials are often prepared via similar chemical strategies to sol−gel superhydrophobics. The characterization of porosity is paramount for these materials and routinely demonstrate the complication of balancing porosity to desired mechanical properties.[120] Aerogels also exhibit distinct similarities in chemistry and are typically prepared in analogous sol−gel reactions. To this end, improving mechanical properties has been a design concern for some time. General design strategies to improve mechanical properties encompass using higher solid contents to increase density directly, promoting particle necking (analogous to Figure 7) or integration of organic polymer networks. A recent spotlight article by Randall et al.[121] outlines these approaches and the recent progress toward robust aerogels. As a consequence the use of aerogel structural motif is attracting more interest toward superhydrophobics.[36]

It could not be expected for all superhydrophobic reports to characterize porosity, given the often complex nature of the material and techniques.[122] Yet at the same time, given the prevalence of voids and porosity within superhydrophobic films, these relations provide one perspective of the underlining challenge toward achieving both a durable and superhydrophobic surface. Further, akin to aerogels, minimizing porosity could be stated as one crucial design consideration.

5. BEAM THEORY

From another perspective, assuming a surface is repeating similar asperities, analyzing a single asperity is a reasonable starting point. A simple geometric approach could be to consider each asperity as an individual pillar and apply conventional Euler beam buckling theory.[123,124]

$$F_{cr} = \frac{\pi^2 EI}{(KL)^2} \tag{5}$$

where F_{cr} is the critical force, E is elastic modulus, I is the moment of inertia, L is the length of the pillar, and K is a factor that describes the support of the pillar; for pillars fixed at one end and one end free, $K = 2$. This model describes the force at which an elastic pillar will buckle based on geometric properties L and I and material property E. In effect, the critical force is inversely proportional to the "fineness" of the pillar. As the aspect ratio increases, which is desirable for minimizing wetting, the rigidity of the pillar is substantially reduced, illustrated in Figure 10.

Beam theory has been applied to many periodic array structures[31,125] including those designed to be superhydrophobic.[30,32,71] Yu et al.[123] utilized this model to study the mechanical durability of lotus leaf structure in regard to withstanding the impact pressure of falling rain drops and hydraulic pressure. The asperities were analyzed through Euler instability where a pillar will become unstable and buckle upon

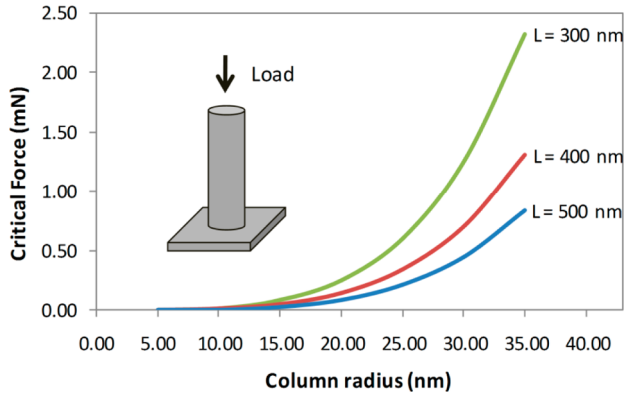

Figure 10. Illustration of cylindrical column considered under Euler beam buckling theory used to describe elastic pillar stability, utilizing a modulus of 72 GPa.

a critical force applied to it. This study arrived at the conclusion that the requirements for superhydrophobicity and mechanical stability are conflicting. Also that hierarchical structure is necessary to meet the mechanical requirement of withstanding heavy rain. Similar theoretical analysis was performed by Wang et al.[126] regarding pillar analysis as above on nanotube forests. It was determined that the forest indentation stiffness scaled linearly with the density of tubes per area, elastic modulus, the radius of the indenter, and the moment of inertia (r^4 for circular cross section) and inversely with the square of nanotube length, as per eq 5. Effectively, durability increases with increased solid to withstand load and with reducing aspect ratio, conflicting with superhydrophobicity requirements.

Asperities considered within this model describe perfect geometric pillars through the moment of inertia variable, I, which is derived from the cross-sectional area of the column. Application to experimental structures is not readily applicable where the cross section is nonuniform,[124] such as the needlelike structure illustrated in Figure 2 where the radius of the structure is reducing toward the film edge, and is nonuniform between asperities. That said, utilizing mean average across a unit cell, approximations have been demonstrated for homogeneous honeycomb structures:[127]

$$I = \frac{bh^3}{12} * (1 - P) \tag{6}$$

where b and h are unit cell lengths, and P is porosity. This provides a key example where porosity will directly reduce buckling resistance through the geometric variable I.

Evaluation of both porosity and beam theory raises concern. First, considering the exponential decrease in E with porosity (eqs 2−4) and then in combination with beam buckling theory in eqs 5 and 6, one could expect a cumulative reduction in resistance, increasingly so as the structure became sharper. Clearly, in isolation or combination of these two approaches for predicting mechanical properties, the structural requirements for achieving superhydrophobicity are exceedingly unfavorable for durability.

In reverse, these relations also present opportunity to dramatically improve mechanical durability by where possible minimizing porosity and minimizing the aspect ratio of surface features. The wettability of periodic structures with varying spacing and aspect ratios has been performed on lithography surfaces,[14] and it is likely there is a window of opportunity[28] to improve mechanical properties while minimizing any com-

promise to wettability through varying aspect ratio and asperity density. Similarly, structures with broadening cross sections (Figures 2 and 9) toward the substrate exhibit improved resistance. This strategy approach was included in the recent report by Park et al.[128] While maintaining the low solid area, the resistance of the overall structure is enhanced. In each case, there will be a threshold at which a loss of wetting properties due to decreasing aspect ratio becomes too severe. In terms of asperity design the hindered load-bearing capacity introduced from (eqs 2−6) also provides additional rationale to shift toward structures with reduced contact pressures[38,101] such as those depicted in Figure 9.

6. INFLUENCE OF SCALE

The discussion of both porosity and beam theory have been discussed as design themes encompassing broad challenges to designing mechanically robust superhydrophobic films. As discussed and witnessed in figures within the report, many superhydrophobic films rely on nanoscale motifs. Owing to the increase in surface area to volume ratios, the quantitative evaluation of both porosity and beam theory becomes more complex and deviates from standard values.[129,130] In fact as size reduces to the order of 10 nm,[131] interfacial stresses can significantly enhance or decrease material properties. This still remains a burgeoning area of research; in particular, complete experimental understanding for complex (i.e., rough) surfaces is still in progress.[132] To this effect these parameters will not be extensively discussed further; however, substantial reviews encompassing investigation of scale-dependency of material properties have been reported.[55,132,133]

7. HIERARCHICAL SURFACES

In most cases superhydrophobic surfaces exhibit hierarchical roughness, typically as both nano and microscopic features. There are many examples reporting the favorability of surfaces with two or more roughness length scales with regard to wetting. In particular, stabilizing the Cassie−Baxter wetting state.[134] This has been postulated as the reasoning behind its presence in natural superhydrophobic surfaces such as the lotus leaf.[123] In the context of mechanical robustness, it has been proposed and demonstrated that relatively larger microscale features withstand more force or even shelter and protect more fragile nanoscale asperities.[13,25,37,135] This effect is often depicted by schematics similar to those in Figure 11. In this

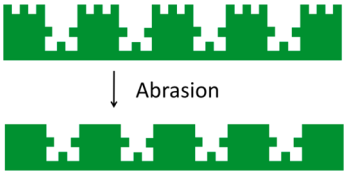

Figure 11. Idealized schematic illustrating the protective nature of microasperities over nanofeatures.

sense, upon the onset of wear, the remaining microroughness and the sheltered nanofeatures may preserve sufficient phobicity. Various methods for producing microroughness include templating,[74] dual-scale particulates,[83,136] substrate roughening (i.e., sandblasting),[137] and lithography.[135]

The immediate concern with utilizing microroughness may be the loss of wetting properties. A recent report by Huoviven et al.[138] studied the shielding capacity of micropillars among nanofeatures of polypropylene surfaces, schematics and images of which are shown in Figure 12.

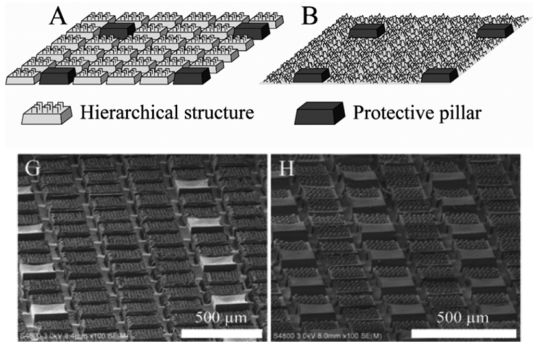

Figure 12. (upper) Schematic representation of protective pillar strategy. (lower) Corresponding example SEMs of surfaces studied by Huviven et al.[138] Reproduced with permission from E. Huovinen, L. Takkunen, T. Korpela, M. Suvanto, T. T. Pakkanen, and T. A. Pakkanen, *Langmuir*, **2014** 30 (5), 1435−1443. Copyright 2014 American Chemical Society.

With increasing fractions of protective pillars the wear resistance increased, to the detriment of wetting properties. The protective density of 15% was determined to be optimal, maintaining superhydrophobic contact angles and increasing resistance to compressive and abrasive forces, 2- and 3-fold, respectively. This engineered arrangement of microfeatures could be repeated for other surface preparations.

However, the performance of this sheltering strategy may vary. In the same manner as the scratch and friction tests mentioned above, the size and speed of the marring body may influence the penetration depth and therefore asperity deformation. Owing to light-scattering effects the scale of microroughness will also be limited[128,139] for films in applications where transparency is vital, that is, windows or solar panels.

Notwithstanding, the benefits of large features can be rationalized from a broad range of perspectives. Depending on the nature of roughness atop of the micron features, the large features diminish contact pressures simply through increased solid area contact. Consequently, in more cases the loading should be less than the yield strength of the material. Further, if these large structures are analyzed from the same beam theory perspective as above it is readily apparent how these microfeatures can yield improved durability and sheltering effects. Ignoring the material properties (E), the traditional buckling formula is dependent on the geometric property—moment area of inertia. These values for common geometries are readily available[124] for which values scale with the length value raised to the fourth power. In the imaginary case of one scale exhibiting length 2 and a second scale had a length of 10, the moments of inertia would include factors of 2^4 and 10^4, respectively. It follows that compared to nano, any microstructure should be considerably more resistant to any failure, which can be governed by cross-sectional area; including buckling or bending. This size relation was also noted by Butt et al.[140] From this perspective it is therefore practical to rely on higher aspect ratio microstructures sheltering lower aspect ratio nanostructures. From another perspective, the source of microroughness is usually a non or minimally porous material. In the case of sand blasting or lithography the material is usually the substrate. Thus, as well as avoiding film adhesion

issues, the porosity difficulties stated above are irrelevant. For particle-constructed films (Figure 6) it could be inferred that reduced particle loadings would be required to achieve sufficient roughness, minimizing any particle loading or porosity issues. Similarly, hierarchically templated craterlike films may allow sufficient roughness at reduced porosities.

8. LESSONS FROM NATURE

Often, nature has provided significant material science inspirations toward material science, superhydrophobicity being one example. Natural superhydrophobic surfaces such as the lotus leaf have attracted considerable characterization and biomimetic strategies.[141] The use of hierarchical roughness akin to the lotus leaf has attracted considerable attention toward its mechanical advantages as discussed above. Unfortunately beyond this, the blueprint for mechanically robust superhydrophobic films is not conveyed in natural surfaces. Given nature's ability to repair itself, the difficulties faced by synthetic thin films are of minimal consequence.

In fact many of these surfaces are constructed by relatively soft materials, and from this perspective pursuing self-healing coatings would be highly desirable. Examples of self-healing superhydrophobic coatings are discussed in reviews by Verho[13] and Xue.[24] In general, the repair is limited to chemical functionality, and repairing surface features remains out of reach. There are some reports that exhibit repeating layers of surface structure whereby the roughness is maintained upon the loss of one or many layers until a minimal film thickness is reached. Some longevity can be achieved utilizing these self-affine structures, such as those presented by Jin et al.[36] Eventually, however, a nonreplenishing surface will entirely diminish.

Removed from superhydrophobicity and the prospect of self-healing, other facets of nature do however provide insight into designing structures to resist mechanical failure. In the same manner as requirements for superhydrophobicity and robustness are conflicting, in general hardness and toughness are also conflicting. This has been a long-term consideration for engineering materials, and conveniently nature has demonstrated how to address this dichotomy through hierarchical design of nano and microscale materials.[142] In a direct sense, for surface architecture, hard and tough asperity is advantageous over hard yet brittle asperity, which may rapidly fail under exacerbated loads. In a theoretical sense this emphasizes rationalizing structures beyond the routine use of two scales and chemical cross-links.

Interestingly, natural materials can achieve both hardness and toughness through clever hierarchical structures utilizing building blocks not too dissimilar to those used to synthetically prepare superhydrophobic films. Replicating these strategies within surface asperities may consequently yield more robust superhydrophobic films.

Biomaterials and their properties have attracted considerable research attention, and many extensive reviews have been reported.[143−145] In general there are some recurring aspects to how nature designs tough materials:[146,147] hybrid composites with anisotropic building blocks and multiple toughening mechanisms.

To contrast one example, a simple sol−gel superhydrophobic coating, which can be prepared using relatively hard, brittle silica isotropic nanoparticles and soft, tough polydimethylsiloxane (PDMS). Nacre, a biocomposite found in mollusc shells, utilizes hard, brittle anisotropic platelets of aragonite and soft protein polymers. The brittle component in nacre constitutes up to 95% of the material, maintaining hardness yet also demonstrating improved toughness.[148] The hierarchical construction allows nacre to surpass the properties of what would be expected for standard composite material. The use of large plates within nacre as a brick and mortar approach produces a large interface between the protein and subsequent plates. This results in significant energy requirement due to friction to dislocate plates, which is further enhanced by nanoasperities between the plates. Owing to the anisotropy and positioning, the plates are mechanically complementary and reinforce one another. In contrast to spherical silica nanoparticles, such mechanisms are not available. The chemistry of the system also exhibits hierarchical toughening mechanisms. To provide toughness nature utilizes soft protein matrix to distribute energy across large areas and prevent failure through energy dissipation mechanisms. Initially upon loading, the "sacrificial"[149] hydrogen bonds are ruptured and expended to unravel protein molecules against entropy prior to more permanent deformation. Mimicking this polymer design has also attracted significant attention.[150] Replicating intricate hierarchical structures is experimentally challenging. Anisotropic building blocks are in general more difficult to prepare, and then controlling aggregation is an additional challenge. More so, completely mimicking such within spray- or spin-coating systems will be a dubious task. Nonetheless, several materials have been reported to mimic nacre structure and exhibit extraordinary properties utilizing ice crystal-templating,[151] alumina platelets,[152] and montmorillonite.[153]

The hierarchical construction of asperities in this manner may be a pathway to improving mechanical robustness. To our knowledge this has not been reported thus far. However, recently, a nacre-like structure prepared utilizing graphene sheets was rendered superhydrophobic with a silica, polystyrene sphere post-treatment.[154] Besides brick and mortar approaches, fiber and fiber bundles[142,143] are frequently used by nature to inhibit crack propagation by bridging interfaces. Fibers,[155] rods,[156] and tubes are anisotropic building blocks, which are more readily obtained and utilized; consequently, the use of fibers has long been utilized in manmade materials, and a wide range of fibrous materials are available.[157,158] Given the scale of features employed in superhydrophobics carbon nanotubes are of particular interest and have been utilized as roughening agents.[159−161] Contributing to roughness, fibers/tubes could promote the hierarchical roughness at reduced porosity levels for surface structures, which are reliant on roughness, which is not protruding from the surface, such as craterlike structures. Reinforcing fibers could be employed to garner long-range internal interface between existing materials, facilitating mechanisms discussed above. Moreover, given the cellular nature of craterlike structures, there is opportunity for fiber reinforcement[162] of the struts between voids, which are most likely to fail under axial loading.

Natural materials highlight the importance of physical structure and exemplify complementary approaches in material construction. As hierarchical construction is routinely used toward improving wetting properties, there is opportunity to explore hierarchically rationalized asperities with capacities to dissipate energy or resist failures.

9. CONCLUSION

The lack of mechanical stability of surface structures is a clear challenge for practical application of superhydrophobic films.

Many superhydrophobic coatings generally fail to adequately address both mechanical and chemical issues. From existing porosity and beam models, eqs 2−5, and corresponding experimental reports, it is recognizable that the requirements for mechanical durability and superhydrophobicity are indeed conflicting. This emphasizes the importance of addressing physical structure in addition to chemical strategies. Specifically, where possible, strategies should encompass minimizing porosity and controlling the geometry of surface features. This will involve a delicate compromise and balance between wetting properties through minimizing water-adhesion points yet maximizing solid content to resist load, for example, needlelike protrusions designed with lower aspect ratios, higher packing density, or avoided entirely in favor of more abrasive resistant craterlike structures. Nature highlights that the manner in which asperities are constructed offers significant opportunity to improve mechanical properties in both complementary geometry and chemical designs. In parallel, mechanical studies encompassing tribological principles are able to provide insight toward asperity failure at relevant length scales through interpretation of friction and scratch profiles. While quantitative measurements are inherently complicated, the utilization of hybrid or in situ nanoindentation is capable of identifying failure dynamics of asperities through manipulation of single asperities, which is a crucial missing element of current characterization.

AUTHOR INFORMATION

Corresponding Author

*Phone: +61 3 8344-6492. Email address: rnlamb@unimelb.edu.au.

Author Contributions

‡These authors contributed equally. The manuscript was written through contributions of all authors. All authors have given approval to the final version of the manuscript.

Notes

The authors declare no competing financial interest.

ACKNOWLEDGMENTS

The financial support of the Australian Research Council's Discovery Projects (Project No. DP120104536) is gratefully acknowledged. The authors also acknowledge Prof. W. Unertl for advice during preparation and K. Nakanishi for providing SEM featured in Figures 2 and 6.

REFERENCES

(1) Fürstner, R.; Barthlott, W.; Neinhuis, C.; Walzel, P. Wetting and Self-Cleaning Properties of Artificial Superhydrophobic Surfaces. *Langmuir* **2005**, *21*, 956−961.

(2) Cao, L.; Jones, A. K.; Sikka, V. K.; Wu, J.; Gao, D. Anti-Icing Superhydrophobic Coatings. *Langmuir* **2009**, *25*, 12444−12448.

(3) Genzer Kirill, J. Recent Developments in Superhydrophobic Surfaces and Their Relevance to Marine Fouling: A Review. *Biofouling* **2006**, *22*, 339−360.

(4) Wu, A.-F.; Nakanishi, K.; Cho, K. L.; Lamb, R. Diatom Attachment Inhibition: Limiting Surface Accessibility through Air Entrapment. *Biointerphases* **2013**, *8*, 1−10.

(5) Young, T. Analysis of Interfacial Forces, London. *Philos. Trans. R. Soc., A* **1805**, *95*, 65.

(6) Wenzel, R. N. Resistance of Solid Surfaces to Wetting by Water. *Ind. Eng. Chem.* **1936**, *28*, 988−994.

(7) Cassie, A. B. D.; Baxter, S. Wettability of Porous Surfaces. *Trans. Faraday Soc.* **1944**, *40*, 546−550.

(8) Bhushan, B. Lotus Effect: Surfaces with Roughness-Induced Superhydrophobicity. In *Springer Handbook of Nanotechnology*; Bhushan, B., Ed.; Springer: Berlin Heidelberg, 2010; pp 1437−1518.

(9) Zhang, X. Superhydrophobic Surfaces: From Structural Control to Functional Application. *J. Mater. Chem.* **2008**, *18*, 621.

(10) Li, X.-M.; Reinhoudt, D.; Crego-Calama, M. What Do We Need for a Superhydrophobic Surface? A Review on the Recent Progress in the Preparation of Superhydrophobic Surfaces. *Chem. Soc. Rev.* **2007**, *36*, 1350−1368.

(11) Nakajima, A.; Hashimoto, K.; Watanabe, T. Recent Studies on Super-Hydrophobic Films. *Monatsh. Chem.* **2001**, *132*, 31−41.

(12) Bhushan, B.; Nosonovsky, M. Scale Effects in Friction Using Strain Gradient Plasticity and Dislocation-Assisted Sliding (microslip). *Acta Mater.* **2003**, *51*, 4331−4345.

(13) Verho, T.; Bower, C.; Andrew, P.; Franssila, S.; Ikkala, O.; Ras, R. H. A. Mechanically Durable Superhydrophobic Surfaces. *Adv. Mater.* **2011**, *23*, 673−678.

(14) Öner, D.; McCarthy, T. J. Ultrahydrophobic Surfaces. Effects of Topography Length Scales on Wettability. *Langmuir* **2000**, *16*, 7777−7782.

(15) Qi, D.; Lu, N.; Xu, H.; Yang, B.; Huang, C.; Xu, M.; Gao, L.; Wang, Z.; Chi, L. Simple Approach to Wafer-Scale Self-Cleaning Antireflective Silicon Surfaces. *Langmuir* **2009**, *25*, 7769−7772.

(16) Hosono, E.; Fujihara, S.; Honma, I.; Zhou, H. Superhydrophobic Perpendicular Nanopin Film by the Bottom-up Process. *J. Am. Chem. Soc.* **2005**, *127*, 13458−13459.

(17) Xu, B.; Cai, Z. Fabrication of a Superhydrophobic ZnO Nanorod Array Film on Cotton Fabrics via a Wet Chemical Route and Hydrophobic Modification. *Appl. Surf. Sci.* **2008**, *254*, 5899−5904.

(18) Li, Y.; Liu, F.; Sun, J. A Facile Layer-by-Layer Deposition Process for the Fabrication of Highly Transparent Superhydrophobic Coatings. *Chem. Commun.* **2009**, 2730−2732.

(19) Zimmermann, J.; Reifler, F. A.; Fortunato, G.; Gerhardt, L.-C.; Seeger, S. A Simple, One-Step Approach to Durable and Robust Superhydrophobic Textiles. *Adv. Funct. Mater.* **2008**, *18*, 3662−3669.

(20) Sas, I.; Gorga, R. E.; Joines, J. A.; Thoney, K. A. Literature Review on Superhydrophobic Self-cleaning Surfaces Produced by Electrospinning. *J. Polym. Sci., Part B: Polym. Phys.* **2012**, *50*, 824−845.

(21) Sanjay, S. L.; Annaso, B. G.; Chavan, S. M.; Rajiv, S. V. Recent Progress in Preparation of Superhydrophobic Surfaces: A Review. *J. Surf. Eng. Mater. Adv. Technol.* **2012**, *2012*.

(22) Roach, P.; Shirtcliffe, N. J.; Newton, M. I. Progess in Superhydrophobic Surface Development. *Soft Matter* **2008**, *4*, 224−240.

(23) Schubert, U.; Huesing, N.; Lorenz, A. Hybrid Inorganic-Organic Materials by Sol-Gel Processing of Organofunctional Metal Alkoxides. *Chem. Mater.* **1995**, *7*, 2010−2027.

(24) Xue, C.-H.; Ma, J.-Z. Long-Lived Superhydrophobic Surfaces. *J. Mater. Chem. A* **2013**, *1*, 4146−4161.

(25) Groten, J.; Rühe, J. Surfaces with Combined Microscale and Nanoscale Structures: A Route to Mechanically Stable Superhydrophobic Surfaces? *Langmuir* **2013**, *29*, 3765−3772.

(26) Zimmermann, J.; Reifler, F. A.; Schrade, U.; Artus, G. R. J.; Seeger, S. Long Term Environmental Durability of a Superhydrophobic Silicone Nanofilament Coating. *Colloids Surf., A* **2007**, *302*, 234−240.

(27) Malavasi, I.; Bernagozzi, I.; Antonini, C.; Marengo, M. Assessing Durability of Superhydrophobic Surfaces. *Surf. Innovations* **2014**, 1−37 DOI: 10.1680/si.14.00001.

(28) Extrand, C. W. Designing for Optimum Liquid Repellency. *Langmuir* **2006**, *22*, 1711−1714.

(29) Tuteja, A.; Choi, W.; Mabry, J. M.; McKinley, G. H.; Cohen, R. E. Robust Omniphobic Surfaces. *Proc. Natl. Acad. Sci. U. S. A.* **2008**, *105*, 18200−18205.

(30) Zhao, H.; Park, K.-C.; Law, K.-Y. Effect of Surface Texturing on Superoleophobicity, Contact Angle Hysteresis, and "Robustness. *Langmuir* **2012**, *28*, 14925−14934.

(31) Chandra, D.; Yang, S. Stability of High-Aspect-Ratio Micropillar Arrays against Adhesive and Capillary Forces. *Acc. Chem. Res.* **2010**, *43*, 1080−1091.
(32) Gogolides, A. Z.; K, E.; A, O.; E. Ultra-High Aspect Ratio Si Nanowires Fabricated with Plasma Etching: Plasma Processing, Mechanical Stability Analysis against Adhesion and Capillary Forces and Oleophobicity. *Nanotechnology* **2014**, *25*, 35302.
(33) Davis, A.; Yeong, Y. H.; Steele, A.; Loth, E.; Bayer, I. S. Spray Impact Resistance of a Superhydrophobic Nanocomposite Coating. *AIChE J.* **2014**, *60*, 3025−3032.
(34) Jung, Y. C.; Bhushan, B. Mechanically Durable Carbon Nanotube-Composite Hierarchical Structures with Superhydrophobicity, Self-Cleaning, and Low-Drag. *ACS Nano* **2009**, *3*, 4155−4163.
(35) Deng, X.; Mammen, L.; Zhao, Y. F.; Lellig, P.; Mullen, K.; Li, C.; Butt, H. J.; Vollmer, D. Transparent, Thermally Stable and Mechanically Robust Superhydrophobic Surfaces Made from Porous Silica Capsules. *Adv. Mater.* **2011**, *23*, 2962−+.
(36) Jin, H.; Tian, X.; Ikkala, O.; Ras, R. H. A. Preservation of Superhydrophobic and Superoleophobic Properties upon Wear Damage. *ACS Appl. Mater. Interfaces* **2013**, *5*, 485−488.
(37) Yonghao, X.; Yan, L.; Dennis, W. H.; Wong, C. P. Mechanically Robust Superhydrophobicity on Hierarchically Structured Si Surfaces. *Nanotechnology* **2010**, *21*, 155705.
(38) Nakajima, A.; Abe, K.; Hashimoto, K.; Watanabe, T. Preparation of Hard Super-Hydrophobic Films with Visible Light Transmission. *Thin Solid Films* **2000**, *376*, 140−143.
(39) Lakshmi, R. V.; Bharathidasan, T.; Basu, B. J. Superhydrophobic Sol-Gel Nanocomposite Coatings with Enhanced Hardness. *Appl. Surf. Sci.* **2011**, *257*, 10421−10426.
(40) Steele, A.; Bayer, I.; Loth, E. Adhesion Strength and Superhydrophobicity of Polyurethane/organoclay Nanocomposite Coatings. *J. Appl. Polym. Sci.* **2012**, *125*, E445−E452.
(41) Boinovich, L. B.; Emelyanenko, A. M.; Ivanov, V. K.; Pashinin, A. S. Durable Icephobic Coating for Stainless Steel. *ACS Appl. Mater. Interfaces* **2013**, *5*, 2549−2554.
(42) Sparks, B. J.; Hoff, E. F. T.; Hayes, L. P.; Patton, D. L. Mussel-Inspired Thiol−Ene Polymer Networks: Influencing Network Properties and Adhesion with Catechol Functionality. *Chem. Mater.* **2012**, *24*, 3633−3642.
(43) Bhushan, B. Mechanical Properties of Nanostructures. In *Nanotribology and Nanomechanics I;* Bhushan, B., Ed.; Springer: Berlin Heidelberg, 2011; pp 527−584.
(44) Bhushan, B. *Modern Tribology Handbook;* CRC Press: Boca Raton, FL, 2001.
(45) Bhushan, B. Mechanical Properties of Nanostructures. In *Springer Handbook of Nanotechnology;* Bhushan, B., Ed.; Springer: Berlin Heidelberg, 2010; pp 1227−1265.
(46) Fischer-Cripps, A. C. *Nanoindentation,* Vol. *1*; Springer: New York, 2011.
(47) Doerner, M. F.; Nix, W. D. A Method for Interpreting the Data from Depth-Sensing Indentation Instrurnents. *J. Mater. Res.* **1986**, *1*.
(48) Oliver, W. C.; Pharr, G. M. Improved Technique for Determining Hardness and Elastic Modulus Using Load and Displacement Sensing Indentation Experiments. *J. Mater. Res.* **1992**, *7*, 1564−1583.
(49) Joslin, D. L.; Oliver, W. C. A New Method for Analyzing Data from Continuous Depth-Sensing Microindentation Tests. *J. Mater. Res.* **1990**, *5*, 123−126.
(50) Bhushan, B.; Li, X. Nanomechanical Characterisation of Solid Surfaces and Thin Films. *Int. Mater. Rev.* **2003**, *48*, 125−164.
(51) Palacio, M. L. B.; Bhushan, B. Depth-Sensing Indentation of Nanomaterials and Nanostructures. *Mater. Charact.* **2013**, *78*, 1−20.
(52) Bhushan, B. Scale Effect in Mechanical Properties and Tribology. In *Springer Handbook of Nanotechnology;* Bhushan, B., Ed.; Springer: Berlin Heidelberg, 2010; pp 1023−1054.
(53) Nix, W. D.; Gao, H. Indentation Size Effects in Crystalline Materials: A Law for Strain Gradient Plasticity. *J. Mech. Phys. Solids* **1998**, *46*, 411−425.
(54) Fleck, N. A.; Muller, G. M.; Ashby, M. F.; Hutchinson, J. W. Strain Gradient Plasticity: Theory and Experiment. *Acta Metall. Mater.* **1994**, *42*, 475−487.
(55) Aston, D. E.; Bow, J. R.; Gangadean, D. N. Mechanical Properties of Selected Nanostructured Materials and Complex Bio-Nano, Hybrid and Hierarchical Systems. *Int. Mater. Rev.* **2013**, *58*, 167−202.
(56) Zhanga, T.-Y.; Xu, W.-H. Surface Effects on Nanoindentation. *J. Mater. Res.* **2002**, *17*, 1716.
(57) Asif, S. A. S.; Colton, R. J.; Wahl, K. J. Nanoscale Surface Mechanical Property Measurements: Force Modulation Techniques Applied to Nanoindentation. In *ACS Symposium Series;* ACS Publications, 2001; Vol. *781*, pp 198−215.
(58) Syed Asif, S. A.; Wahl, K. J.; Colton, R. J.; Warren, O. L. Quantitative Imaging of Nanoscale Mechanical Properties Using Hybrid Nanoindentation and Force Modulation. *J. Appl. Phys.* **2001**, *90*, 1192−1200.
(59) Asif, S. A.; Wahl, K. J.; Colton, R. J. Nanoindentation and Contact Stiffness Measurement Using Force Modulation with a Capacitive Load-Displacement Transducer. *Rev. Sci. Instrum.* **1999**, *70*, 2408−2413.
(60) Bei, H.; Shim, S.; George, E. P.; Miller, M. K.; Herbert, E. G.; Pharr, G. M. Compressive Strengths of Molybdenum Alloy Micro-Pillars Prepared Using a New Technique. *Scr. Mater.* **2007**, *57*, 397−400.
(61) Frick, C. P.; Clark, B. G.; Orso, S.; Schneider, A. S.; Arzt, E. Size Effect on Strength and Strain Hardening of Small-Scale [111] Nickel Compression Pillars. *Mater. Sci. Eng., A* **2008**, *489*, 319−329.
(62) Moser, B.; Wasmer, K.; Barbieri, L.; Michler, J. Strength and Fracture of Si Micropillars: A New Scanning Electron Microscopy-Based Micro-Compression Test. *J. Mater. Res.* **2007**, *22*, 1004−1011.
(63) Philippe, L.; Peyrot, I.; Michler, J.; Hassel, A. W.; Milenkovic, S. Yield Stress of Monocrystalline Rhenium Nanowires. *Appl. Phys. Lett.* **2007**, *91*, 111919.
(64) Nili, H.; Kalantar-zadeh, K.; Bhaskaran, M.; Sriram, S. In Situ Nanoindentation: Probing Nanoscale Multifunctionality. *Prog. Mater. Sci.* **2013**, *58*, 1−29.
(65) Bhushan, B. Nanotribology, Nanomechanics and Nanomaterials Characterization. *Philos. Trans. R. Soc., A* **2008**, *366*, 1351−1381.
(66) Bhushan, B. Surface Forces and Nanorheology of Molecularly Thin Films. In *Springer Handbook of Nanotechnology;* Bhushan, B., Ed.; Springer: Berlin Heidelberg, 2010; pp 857−911.
(67) Kim, H.-J.; Kim, D.-E. Nano-Scale Friction: A Review. *Int. J. Precis. Eng. Manuf.* **2009**, *10*, 141−151.
(68) Leyland, A.; Matthews, A. On the Significance of The H/ E Ratio in Wear Control: A Nanocomposite Coating Approach to Optimised Tribological Behaviour. *Wear* **2000**, *246*, 1−11.
(69) Leyland, A.; Matthews, A. Optimization of Nanostructured Tribological Coatings. In *Nanostructured Coatings;* Springer:New York, 2006; pp 511−538.
(70) Skarmoutsou, A.; Charitidis, C. A.; Gnanappa, A. K.; Tserepi, A.; Gogolides, E. Nanomechanical and Nanotribological Properties of Plasma Nanotextured Superhydrophilic and Superhydrophobic Polymeric Surfaces. *Nanotechnology* **2012**, *23*, 505711.
(71) Ellinas, K.; Pujari, S. P.; Dragatogiannis, D. A.; Charitidis, C. A.; Tserepi, A.; Zuilhof, H.; Gogolides, E. Plasma Micro-Nanotextured, Scratch, Water and Hexadecane Resistant, Superhydrophobic, and Superamphiphobic Polymeric Surfaces with Perfluorinated Monolayers. *ACS Appl. Mater. Interfaces* **2014**, *6*, 6510−6524.
(72) Brinker, C. J.; Scherer, G. W. *Sol-Gel Science: The Physics and Chemistry of Sol-Gel Processing;* Academic Press, Boston, MA, 1990.
(73) Wen, J.; Wilkes, G. L. Organic/inorganic Hybrid Network Materials by the Sol-Gel Approach. *Chem. Mater.* **1996**, *8*, 1667−1681.
(74) Cho, K. L.; Liaw, I. I.; Wu, A. H.-F.; Lamb, R. N. Influence of Roughness on a Transparent Superhydrophobic Coating. *J. Phys. Chem. C* **2010**, *114*, 11228−11233.
(75) Zhang, H.; Lamb, R.; Jones, A. (Unisearch Limited, AU). Durable Superhydrophobic Coating. US Patent 2,004,090,065, A1, April 8, 2004.

(76) Paul, D. R.; Robeson, L. M. Polymer Nanotechnology: Nanocomposites. *Polymer* **2008**, *49*, 3187−3204.
(77) Walter, R.; Rong, M.; Zhang, M.; Zheng, Y.; Zeng, H.; Friedrich, K. Structure−property Relationships of Irradiation Grafted Nano-Inorganic Particle Filled Polypropylene Composites. *Polymer* **2001**, *42*, 167−183.
(78) Jordan, J.; Jacob, K. I.; Tannenbaum, R.; Sharaf, M. A.; Jasiuk, I. Experimental Trends in Polymer Nanocomposites—a Review. *Mater. Sci. Eng., A* **2005**, *393*, 1−11.
(79) Wetzel, B.; Haupert, F.; Qiu Zhang, M. Epoxy Nanocomposites with High Mechanical and Tribological Performance. *Compos. Sci. Technol.* **2003**, *63*, 2055−2067.
(80) Fu, S.-Y.; Feng, X.-Q.; Lauke, B.; Mai, Y.-W. Effects of Particle Size, Particle/matrix Interface Adhesion and Particle Loading on Mechanical Properties of Particulate−polymer Composites. *Composites, Part B* **2008**, *39*, 933−961.
(81) Takadoum, J. *Nanomaterials and Surface Engineering;* Wiley: London, U.K., 2013.
(82) Lamb, R.; Zhang, H.; Raston, C. (Unisearch Limited, AU). Hydrophobic Coatings; Au. Pat.,97−5789, 1997. *PCT Int. Appl.* WO1998042452 A1, 1998.
(83) Ming, W.; Wu, D.; van Benthem, R.; de With, G. Superhydrophobic Films from Raspberry-like Particles. *Nano Lett.* **2005**, *5*, 2298−2301.
(84) Wu, G.-Y.; Wang, S.-S.; Wu, J.-C.; Hsu, M.-Y.; Chen, H. Preparation of Highly Adhesive and Superhydrophobic Epoxy-Based Thin Film by Sol−Gel Process. *J. Adhes. Sci. Technol.* **2011**, *25*, 1095−1106.
(85) Bayer, I. S.; Brown, A.; Steele, A.; Loth, E. Transforming Anaerobic Adhesives into Highly Durable and Abrasion Resistant Superhydrophobic Organoclay Nanocomposite Films: A New Hybrid Spray Adhesive for Tough Superhydrophobicity. *Appl. Phys. Express* **2009**, *2*, 5003.
(86) Manca, M.; Cannavale, A.; De Marco, L.; Arico, A. S.; Cingolani, R.; Gigli, G. Durable Superhydrophobic and Antireflective Surfaces by Trimethylsilanized Silica Nanoparticles-Based Sol-Gel Processing. *Langmuir* **2009**, *25*, 6357−6362.
(87) Daoud, W. A.; Xin, J. H.; Tao, X. Superhydrophobic Silica Nanocomposite Coating by a Low-Temperature Process. *J. Am. Ceram. Soc.* **2004**, *87*, 1782−1784.
(88) Taurino, R.; Fabbri, E.; Messori, M.; Pilati, F.; Pospiech, D.; Synytska, A. Facile Preparation of Superhydrophobic Coatings by Sol−gel Processes. *J. Colloid Interface Sci.* **2008**, *325*, 149−156.
(89) Shang, H. M.; Wang, Y.; Limmer, S. J.; Chou, T. P.; Takahashi, K.; Cao, G. Z. Optically Transparent Superhydrophobic Silica-Based Films. *Thin Solid Films* **2005**, *472*, 37−43.
(90) Ma, M.; Hill, R. M. Superhydrophobic Surfaces. *Curr. Opin. Colloid Interface Sci.* **2006**, *11*, 193−202.
(91) Hikita, M.; Tanaka, K.; Nakamura, T.; Kajiyama, T.; Takahara, A. Super-Liquid-Repellent Surfaces Prepared by Colloidal Silica Nanoparticles Covered with Fluoroalkyl Groups. *Langmuir* **2005**, *21*, 7299−7302.
(92) King, S. W.; Bielefeld, J.; Xu, G.; Lanford, W. A.; Matsuda, Y.; Dauskardt, R. H.; Kim, N.; Hondongwa, D.; Olasov, L.; Daly, B.; et al. Influence of Network Bond Percolation on the Thermal, Mechanical, Electrical and Optical Properties of High and Low-K a-SiC:H Thin Films. *J. Non-Cryst. Solids* **2013**, *379*, 67−79.
(93) Guo, Z. G.; Liang, J.; Fang, J.; Guo, B. G.; Liu, W. M. A Novel Approach to the Robust Ti6Al4V-Based Superhydrophobic Surface with Crater-like Structure. *Adv. Eng. Mater.* **2007**, *9*, 316−321.
(94) Widawski, G.; Rawiso, M.; François, B. Self-Organized Honeycomb Morphology of Star-Polymer Polystyrene Films. *Nature* **1994**, *369*, 387−389 DOI: 10.1038/369387a0.
(95) Yabu, H.; Takebayashi, M.; Tanaka, M.; Shimomura, M. Superhydrophobic and Lipophobic Properties of Self-Organized Honeycomb and Pincushion Structures. *Langmuir* **2005**, *21*, 3235−3237.
(96) Yanagisawa, T.; Nakajima, A.; Sakai, M.; Kameshima, Y.; Okada, K. Preparation and Abrasion Resistance of Transparent Super-Hydrophobic Coating by Combining Crater-like Silica Films with Acicular Boehmite Powder. *Mater. Sci. Eng., B* **2009**, *161*, 36−39.
(97) Han, K. D.; Leo, C. P.; Chai, S. P. Fabrication and Characterization of Superhydrophobic Surface by Using Water Vapor Impingement Method. *Appl. Surf. Sci.* **2012**, *258*, 6739−6744.
(98) Kaune, G.; Memesa, M.; Meier, R.; Ruderer, M. A.; Diethert, A.; Roth, S. V.; D'Acunzi, M.; Gutmann, J. S.; Muller-Buschbaum, P. Hierarchically Structured Titania Films Prepared by Polymer/colloidal Templating. *ACS Appl. Mater. Interfaces* **2009**, *1*, 2862−2869.
(99) Brown, P. S.; Talbot, E. L.; Wood, T. J.; Bain, C. D.; Badyal, J. P. S. Superhydrophobic Hierarchical Honeycomb Surfaces. *Langmuir* **2012**, *28*, 13712−13719.
(100) Dyett, B. P.; Wu, A. H.; Lamb, R. N. Toward Superhydrophobic and Durable Coatings: Effect of Needle vs Crater Surface Architecture. *ACS Appl. Mater. Interfaces* **2014**, *6*, 9503−9507.
(101) Kim, J.; Choi, H. J.; Park, K.; Cohen, R. E.; McKinley, G. H.; Barbastathis, G. Multifunctional Inverted Nanocone Arrays for Non-wetting, Self-cleaning Transparent Surface with High Mechanical Robustness. *Small* **2014**, *10*, 2487−2494.
(102) Gibson, L. J.; Ashby, M. F. *Cellular Solids: Structure and Properties;* Cambridge University Press: Cambridge, U.K., 1999.
(103) Gibson, L. J.; Ashby, M. F. The Mechanics of Three-Dimensional Cellular Materials. *Proc. R. Soc. London., Ser. A.* **1982**, *382*, 43−59.
(104) Phani, K. K.; Niyogi, S. K. Elastic Modulus-Porosity Relation in Polycrystalline Rare-Earth Oxides. *J. Am. Ceram. Soc.* **1987**, *70*, C−362−C−366.
(105) Vella, J. B.; Adhihetty, I. S.; Junker, K.; Volinsky, A. A. Mechanical Properties and Fracture Toughness of Organo-Silicate Glass (OSG) Low-K Dielectric Thin Films for Microelectronic Applications. *Int. J. Fract.* **2003**, *120*, 487−499.
(106) Woignier, T.; Reynes, J.; Alaoui, A. H.; Beurroies, I.; Phalippou, J. Different Kinds of Structure in Aerogels: Relationships with the Mechanical Properties. *J. Non-Cryst. Solids* **1998**, *241*, 45−52.
(107) Silva, M. J.; Gibson, L. J. The Effects of Non-Periodic Microstructure and Defects on the Compressive Strength of Two-Dimensional Cellular Solids. *Int. J. Mech. Sci.* **1997**, *39*, 549−563.
(108) Bellet, D.; Lamagnere, P.; Vincent, A.; Brechet, Y. Nano-indentation Investigation of the Young's Modulus of Porous Silicon. *J. Appl. Phys.* **1996**, *80*, 3772−3776.
(109) Díaz, A.; Hampshire, S. Characterisation of Porous Silicon Nitride Materials Produced with Starch. *J. Eur. Ceram. Soc.* **2004**, *24*, 413−419.
(110) Jain, A.; Rogojevic, S.; Ponoth, S.; Agarwal, N.; Matthew, I.; Gill, W. N.; Persans, P.; Tomozawa, M.; Plawsky, J. L.; Simonyi, E. Porous Silica Materials as Low-K Dielectrics for Electronic and Optical Interconnects. *Thin Solid Films* **2001**, *398*, 513−522.
(111) Ashkin, D.; Haber, R. A.; Wachtman, J. B. Elastic Properties of Porous Silica Derived from Colloidal Gels. *J. Am. Ceram. Soc.* **1990**, *73*, 3376−3381.
(112) Spriggs, R. M. Expression for Effect of Porosity on Elastic Modulus of Polycrystalline Refractory Materials, Particularly Aluminum Oxide. *J. Am. Ceram. Soc.* **1961**, *44*, 628−629.
(113) Rice, R. W. Comparison of Physical Property Porosity Behaviour with Minimum Solid Area Models. *J. Mater. Sci.* **1996**, *31*, 1509−1528.
(114) Rice, R. W. Comparison of Stress Concentration versus Minimum Solid Area Based Mechanical Property-Porosity Relations. *J. Mater. Sci.* **1993**, *28*, 2187−2190.
(115) Williford, R. E.; Li, X. S.; Addleman, R. S.; Fryxell, G. E.; Baskaran, S.; Birnbaum, J. C.; Coyle, C.; Zemanian, T. S.; Wang, C.; Courtney, A. R. Mechanical Stability of Templated Mesoporous Silica Thin Films. *Microporous Mesoporous Mater.* **2005**, *85*, 260−266.
(116) Wang, S.; Ngan, A. H. W.; Ng, K. Y. Anomalous Load Dependence in Single-Asperity Tribological Behaviour of Anodic Aluminium Oxide Nanohoneycombs. *Scr. Mater.* **2012**, *67*, 360−363.
(117) Ng, K. Y.; Ngan, A. H. W. Effects of Pore-Channel Ordering on the Mechanical Properties of Anodic Aluminum Oxide Nano-Honeycombs. *Scr. Mater.* **2012**, *66*, 439−442.

(118) Ko, S. H.; Lee, D. W.; Jee, S. E.; Park, H. C.; Lee, K. H.; Hwang, W. Mechanical Properties and Residual Stress Measurements in Anodic Aluminium Oxide Structures Using Nanoindentation. *Glass Phys. Chem.* **2005**, *31*, 356−363.
(119) Dukhyun, C.; Sangmin, L.; Changwoo, L.; Pyungsoo, L.; Junghyun, L.; Kunhong, L.; Hyunchul, P.; Woonbong, H. Dependence of the Mechanical Properties of Nanohoneycomb Structures on Porosity. *J. Micromech. Microeng.* **2007**, *17*, 501.
(120) Maex, K.; Baklanov, M. R.; Shamiryan, D.; Brongersma, S. H.; Yanovitskaya, Z. S. Low Dielectric Constant Materials for Microelectronics. *J. Appl. Phys.* **2003**, *93*, 8793−8841.
(121) Randall, J. P.; Meador, M. A. B.; Jana, S. C. Tailoring Mechanical Properties of Aerogels for Aerospace Applications. *ACS Appl. Mater. Interfaces* **2011**, *3*, 613−626.
(122) Rouquerol, J.; Avnir, D.; Fairbridge, C. W.; Everett, D. H.; Haynes, J. M.; Pernicone, N.; Ramsay, J. D. F.; Sing, K. S. W.; Unger, K. K. Recommendations for the Characterization of Porous Solids (Technical Report). *Pure Appl. Chem.* **1994**, *66*, 1739−1758.
(123) Yu, Y.; Zhao, Z.-H.; Zheng, Q.-S. Mechanical and Superhydrophobic Stabilities of Two-Scale Surfacial Structure of Lotus Leaves. *Langmuir* **2007**, *23*, 8212−8216.
(124) Beer, F. P.; Johnston, E. R.; DeWolf, J. T.; Mazurek, D. F.*Mechanics of Materials;* McGraw Hill: New Delhi, India, 2010.
(125) Glassmaker, N. J.; Jagota, A.; Hui, C.-Y.; Kim, J. Design of Biomimetic Fibrillar Interfaces: 1. Making Contact. *J. R. Soc., Interface* **2004**, *1*, 23−33.
(126) Wang, L.; Ortiz, C.; Boyce, M. C. Mechanics of Indentation into Micro-and Nanoscale Forests of Tubes, Rods, or Pillars. *J. Eng. Mater. Technol.* **2010**, *133*, 011014.
(127) Choi, D.; Jeon, J.; Lee, P.; Hwang, W.; Lee, K.; Park, H. Young's Modulus Measurements of Nanohoneycomb Structures by Flexural Testing in Atomic Force Microscopy. *Compos. Struct.* **2007**, *79*, 548−553.
(128) Park, K.-C.; Choi, H. J.; Chang, C.-H.; Cohen, R. E.; McKinley, G. H.; Barbastathis, G. Nanotextured Silica Surfaces with Robust Superhydrophobicity and Omnidirectional Broadband Supertransmissivity. *ACS Nano* **2012**, *6*, 3789−3799.
(129) Wang, G.-F.; Feng, X.-Q. Surface Effects on Buckling of Nanowires under Uniaxial Compression. *Appl. Phys. Lett.* **2009**, *94*, 141913.
(130) Feng, X.-Q.; Xia, R.; Li, X.; Li, B. Surface Effects on the Elastic Modulus of Nanoporous Materials. *Appl. Phys. Lett.* **2009**, *94*, 011916.
(131) Cammarata, R. C. Surface and Interface Stress Effects in Thin Films. *Prog. Surf. Sci.* **1994**, *46*, 1−38.
(132) Wang, J.; Huang, Z.; Duan, H.; Yu, S.; Feng, X.; Wang, G.; Zhang, W.; Wang, T. Surface Stress Effect in Mechanics of Nanostructured Materials. *Acta Mech. Solida Sin. (Chin. Ed.)* **2011**, *24*, 52−82.
(133) Sun, C. Q. Thermo-Mechanical Behavior of Low-Dimensional Systems: The Local Bond Average Approach. *Prog. Mater. Sci.* **2009**, *54*, 179−307.
(134) Nosonovsky, M. Multiscale Roughness and Stability of Superhydrophobic Biomimetic Interfaces. *Langmuir* **2007**, *23*, 3157−3161.
(135) Huovinen, E.; Hirvi, J.; Suvanto, M.; Pakkanen, T. A. Micro−micro Hierarchy Replacing Micro−nano Hierarchy: A Precisely Controlled Way to Produce Wear-Resistant Superhydrophobic Polymer Surfaces. *Langmuir* **2012**, *28*, 14747−14755.
(136) Ebert, D.; Bhushan, B. Durable Lotus-Effect Surfaces with Hierarchical Structure Using Micro- and Nanosized Hydrophobic Silica Particles. *J. Colloid Interface Sci.* **2012**, *368*, 584−591.
(137) Cui, Z.; Yin, L.; Wang, Q.; Ding, J.; Chen, Q. A Facile Dip-Coating Process for Preparing Highly Durable Superhydrophobic Surface with Multi-Scale Structures on Paint Films. *J. Colloid Interface Sci.* **2009**, *337*, 531−537.
(138) Huovinen, E.; Takkunen, L.; Korpela, T.; Suvanto, M.; Pakkanen, T. T.; Pakkanen, T. A. Mechanically Robust Superhydrophobic Polymer Surfaces Based on Protective Micropillars. *Langmuir* **2014**, *30*, 1435−1443.
(139) Wang, C.; Wu, A. H. F.; Lamb, R. N. Superhydrophobicity and Optical Transparency in Thin Films: Criteria for Coexistence. *J. Phys. Chem. C* **2014**, *118*, 5328−5335.
(140) Butt, H.-J.; Semprebon, C.; Papadopoulos, P.; Vollmer, D.; Brinkmann, M.; Ciccotti, M. Design Principles for Superamphiphobic Surfaces. *Soft Matter* **2013**, *9*, 418−428.
(141) Guo, Z.; Liu, W.; Su, B.-L. Superhydrophobic Surfaces: From Natural to Biomimetic to Functional. *J. Colloid Interface Sci.* **2011**, *353*, 335−355.
(142) Ritchie, R. O. The Conflicts between Strength and Toughness. *Nat. Mater.* **2011**, *10*, 817−822.
(143) Fratzl, P.; Weinkamer, R. Nature's Hierarchical Materials. *Prog. Mater. Sci.* **2007**, *52*, 1263−1334.
(144) Meyers, M. A.; Chen, P.-Y.; Lin, A. Y.-M.; Seki, Y. Biological Materials: Structure and Mechanical Properties. *Prog. Mater. Sci.* **2008**, *53*, 1−206.
(145) Meyers, M. A.; Chen, P.-Y.; Lopez, M. I.; Seki, Y.; Lin, A. Y. M. Biological Materials: A Materials Science Approach. *J. Mech. Behav. Biomed. Mater.* **2011**, *4*, 626−657.
(146) Meyers, M. A.; McKittrick, J.; Chen, P.-Y. Structural Biological Materials: Critical Mechanics-Materials Connections. *Science* **2013**, *339*, 773−779.
(147) Gao, H.; Ji, B.; Jäger, I. L.; Arzt, E.; Fratzl, P. Materials Become Insensitive to Flaws at Nanoscale: Lessons from Nature. *Proc. Natl. Acad. Sci. U. S. A.* **2003**, *100*, 5597−5600.
(148) Espinosa, H. D.; Juster, A. L.; Latourte, F. J.; Loh, O. Y.; Gregoire, D.; Zavattieri, P. D. Tablet-Level Origin of Toughening in Abalone Shells and Translation to Synthetic Composite Materials. *Nat. Commun.* **2011**, *2*, 173.
(149) Fantner, G. E.; Oroudjev, E.; Schitter, G.; Golde, L. S.; Thurner, P.; Finch, M. M.; Turner, P.; Gutsmann, T.; Morse, D. E.; Hansma, H. Sacrificial Bonds and Hidden Length: Unraveling Molecular Mesostructures in Tough Materials. *Biophys. J.* **2006**, *90*, 1411−1418.
(150) Kushner, A. M.; Guan, Z. Modular Design in Natural and Biomimetic Soft Materials. *Angew. Chem., Int. Ed.* **2011**, *50*, 9026−9057.
(151) Munch, E.; Launey, M. E.; Alsem, D. H.; Saiz, E.; Tomsia, A. P.; Ritchie, R. O. Tough, Bio-Inspired Hybrid Materials. *Science* **2008**, *322*, 1516−1520.
(152) Erb, R. M.; Libanori, R.; Rothfuchs, N.; Studart, A. R. Composites Reinforced in Three Dimensions by Using Low Magnetic Fields. *Science* **2012**, *335*, 199−204.
(153) Luz, G. M.; Mano, J. F. Biomimetic Design of Materials and Biomaterials Inspired by the Structure of Nacre. *Philos. Trans. R. Soc., A* **2009**, *367*, 1587−1605.
(154) Zhong, D.; Yang, Q.; Guo, L.; Dou, S.; Liu, K.; Jiang, L. Fusion of Nacre, Mussel, and Lotus Leaf: Bio-Inspired Graphene Composite Paper with Multifunctional Integration. *Nanoscale* **2013**, *5*, 5758−5764.
(155) Doshi, J.; Reneker, D. H. Electrospinning Process and Applications of Electrospun Fibers. *J. Electrostat.* **1995**, *35*, 151−160.
(156) Kuijk, A.; van Blaaderen, A.; Imhof, A. Synthesis of Monodisperse, Rodlike Silica Colloids with Tunable Aspect Ratio. *J. Am. Chem. Soc.* **2011**, *133*, 2346−2349.
(157) Breuer, O.; Sundararaj, U. Big Returns from Small Fibers: A Review of Polymer/carbon Nanotube Composites. *Polym. Compos.* **2004**, *25*, 630−645.
(158) Liu, Y.; Kumar, S. Polymer/Carbon Nanotube Nano Composite Fibers−A Review. *ACS Appl. Mater. Interfaces* **2014**, *6*, 6069−6087.
(159) Lau, K. K. S.; Bico, J.; Teo, K. B. K.; Chhowalla, M.; Amaratunga, G. A. J.; Milne, W. I.; McKinley, G. H.; Gleason, K. K. Superhydrophobic Carbon Nanotube Forests. *Nano Lett.* **2003**, *3*, 1701−1705.
(160) Jung, Y. C.; Bhushan, B. Mechanically Durable Carbon Nanotube−Composite Hierarchical Structures with Superhydrophobicity, Self-Cleaning, and Low-Drag. *ACS Nano* **2009**, *3*, 4155−4163.

(161) Han, J. T.; Kim, S. Y.; Woo, J. S.; Lee, G.-W. Transparent, Conductive, and Superhydrophobic Films from Stabilized Carbon Nanotube/Silane Sol Mixture Solution. *Adv. Mater.* **2008**, *20*, 3724−3727.
(162) Meador, M. A. B.; Vivod, S. L.; McCorkle, L.; Quade, D.; Sullivan, R. M.; Ghosn, L. J.; Clark, N.; Capadona, L. A. Reinforcing Polymer Cross-Linked Aerogels with Carbon Nanofibers. *J. Mater. Chem.* **2008**, *18*, 1843−1852.